CrossMark

Analysis of Monoclonal Antibodies in Human Serum as a Model for Clinical Monoclonal Gammopathy by Use of 21 Tesla FT-ICR Top-Down and Middle-Down MS/MS

Lidong He,[1] Lissa C. Anderson,[2] David R. Barnidge,[3] David L. Murray,[3]
Christopher L. Hendrickson,[1,2] Alan G. Marshall[1,2]

[1]Department of Chemistry and Biochemistry, Florida State University, Tallahassee, FL 32310, USA
[2]National High Magnetic Field Laboratory, Florida State University, 1800 East Paul Dirac Dr., Tallahassee, FL 32310, USA
[3]Department of Laboratory Medicine and Pathology, Mayo Clinic, Rochester, MN 55905, USA
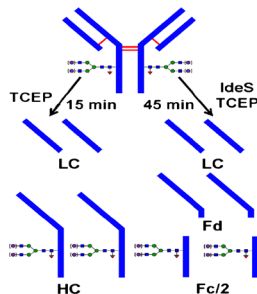
Abstract. With the rapid growth of therapeutic monoclonal antibodies (mAbs), stringent quality control is needed to ensure clinical safety and efficacy. Monoclonal antibody primary sequence and post-translational modifications (PTM) are conventionally analyzed with labor-intensive, bottom-up tandem mass spectrometry (MS/MS), which is limited by incomplete peptide sequence coverage and introduction of artifacts during the lengthy analysis procedure. Here, we describe top-down and middle-down approaches with the advantages of fast sample preparation with minimal artifacts, ultrahigh mass accuracy, and extensive residue cleavages by use of 21 tesla FT-ICR MS/MS. The ultrahigh mass accuracy yields an RMS error of 0.2–0.4 ppm for antibody light chain, heavy chain, heavy chain Fc/2, and Fd subunits. The corresponding sequence coverages are 81%, 38%, 72%, and 65% with MS/MS RMS error ~4 ppm. Extension to a monoclonal antibody in human serum as a monoclonal gammopathy model yielded 53% sequence coverage from two nano-LC MS/MS runs. A blind analysis of five therapeutic monoclonal antibodies at clinically relevant concentrations in human serum resulted in correct identification of all five antibodies. Nano-LC 21 T FT-ICR MS/MS provides nonpareil mass resolution, mass accuracy, and sequence coverage for mAbs, and sets a benchmark for MS/MS analysis of multiple mAbs in serum. This is the first time that extensive cleavages for both variable and constant regions have been achieved for mAbs in a human serum background.

Keywords: Fourier transform, Ion cyclotron resonance, FTMS, Electrospray, MS/MS, Middle-down, Collision-induced dissociation, CID, Electron transfer dissociation, ETD, Multiple myeloma, Isotype, Variable region

Introduction

Therapeutic monoclonal antibodies (mAbs) constitute the fastest growing human therapeutics market class in recent years [1]. More than 40 mAbs have been approved by the US Food and Drug Administration (FDA) and European Medicine

---

The original version of this article was revised to use the corrected version of Figure 6.

Electronic supplementary material The online version of this article (doi:10. 1007/s13361-017-1602-6) contains supplementary material, which is available to authorized users.

Correspondence to: Alan G. Marshall; *e-mail:* marshall@magnet.fsu.edu

---

Agency (EMA) for therapeutic use [2]. These mAbs can be directly applied to treatment of cancer [3] and autoimmune diseases such as rheumatoid arthritis, Crohn's disease, and ulcerative colitis [4]. They can also be conjugated with drugs so that the cytotoxic effect from the drug can be targeted at malignant cells [5].

An antibody consists of two identical light chains (each ~25 kDa) and two identical heavy chains (each ~50 kDa) held together by disulfide bonds. There are two light chain isotypes (κ and λ) and five heavy chain isotypes (α, δ, γ, ε, and μ). Light chains and heavy chains contain an N-terminal variable region and C-terminal constant region. The amino acid sequence in the variable region is unique to each B-cell and is responsible for binding to a specific antigen, whereas the constant region is

virtually identical for each isotype and initiates antibody-dependent, cell-mediated cytotoxicity (ADCC) [6–8]. To ensure safety and efficacy, therapeutic mAb primary sequence and post-translational modifications such as oxidation, deamidation, N-glycosylation, and heavy chain C-terminal lysine clipping are required for full characterization [1].

Bottom-up liquid chromatography-tandem mass spectrometry (LC-MS/MS) is widely used for mAb characterization [9–14]. That approach requires antibody reduction, alkylation, and enzymatic digestion, which are labor-intensive and introduce artifactual heterogeneities during lengthy sample preparation [15]. Alternatively, intact mAb top-down LC-MS/MS offers the advantages of fast sample preparation and minimal artifacts [16–20]. However, the sequence coverage with electron transfer dissociation (ETD) and collision induced dissociation (CID) decreases dramatically for large proteins. Thus, a middle-down approach beginning with limited proteolysis of a large protein produces subunits that are more amenable to MS/MS analysis [21, 22]. Direct mAb disulfide bond reduction yields free light chains and heavy chains. The immunoglobulin G-degrading enzyme from *Streptococcus pyogenes* (IdeS) specifically cleaves mAb at the hinge region, generating three unique ~25 kDa subunits (Fc/2, LC, and Fd) after disulfide bond reduction for MS/MS analysis (Figure 1) [23].

Here, we describe the application of nano-LC 21 tesla FT-ICR MS, top-down MS/MS (light chain, heavy chain), and middle-down (light chain, heavy chain Fc/2, and Fd subunits after protease digestion) MS/MS to characterize therapeutic monoclonal antibody with ultrahigh mass accuracy and extensive residue cleavages. This method detects, characterizes, and quantitates mAb in human serum at concentrations corresponding to those in patients with monoclonal gammopathy. The concentrations in our monoclonal gammopathy model (see below) extend from 0.2 to 16.9 μM. Furthermore, successful blind identification of each of five therapeutic monoclonal antibodies in human serum shows the potential of this approach for future analysis of monoclonal antibodies in clinical samples. Mass error from the software (Xtract and THRASH) deconvolution is discussed, and deconvolution algorithm optimization is needed to match the low mass error from the 21 T FT-ICR MS/MS.

Experimental

Materials

Human serum was purchased from EMD Millipore (Billerica, MA, USA). All therapeutic mAbs were obtained from the Mayo Clinic pharmacy. Tris(2-carboxyethyl)phosphine hydrochloride (TCEP-HCl), myoglobin, acetic acid (≥99.99%), and isopropyl alcohol (LCMS grade) were acquired from Sigma-Aldrich (St. Louis, MO, USA). Water (LCMS grade) and acetonitrile (ACN, LCMS grade) were obtained from Honeywell Burdick and Jackson (Muskegon, MI, USA).

Immunoglobulin Reduction

Immunoglobulins were purified from human serum by use of Melon Gel (Thermo Fisher Scientific, Waltham, MA, USA)
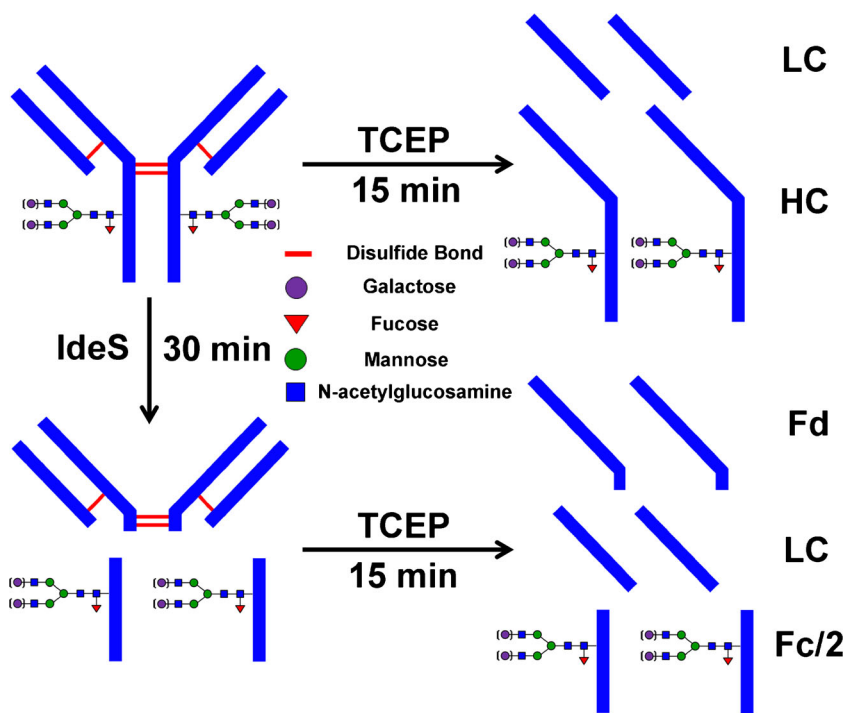
Figure 1. Scheme for (light chain (LC), heavy chain (HC)) and middle-down (light chain, heavy chain Fc/2, and Fd subunits after protease digestion) top-down MS/MS to characterize therapeutic monoclonal antibodies

according to the manufacturer's protocol and further desalted with an Amicon Ultra-0.5 Centrifugal Filter Unit with Ultracel-10 k (10 kDa molecular weight cutoff) membrane (EMD Millipore, Darmstadt, Germany). Final volume was ~20 μL. Eleven μL 10 mM TCEP in 0.1% (v/v) acetic acid in water was added to 1 μL sample and incubated at 75 °C for 15 min to produce intact antibody light (~24 kDa) and heavy (~50 kDa) chains. For pure monoclonal immunoglobulin analysis (no human serum), adalimumab was reduced with 10 mM TCEP directly. Samples were acidified with 228 μL 1% (v/v) acetic acid to pH ~2 prior to nano-LC ESI MS/MS analysis.

Immunoglobulin IdeS Digestion and Reduction

One unit of IdeS (FabRICATOR; Genovis, Cambridge, MA, USA) was added per microgram of IgG and incubated at 10 μg/μL at 37 °C for 30 min as instructed by the manufacturer. Following digestion, samples were reduced with TCEP and acidified as described above. The effects of these treatments are shown schematically in Figure 1.

Liquid Chromatography and Mass Spectrometry Conditions

A Waters Acquity UPLC M-Class System (Milford, MA, USA) was used for separation. A custom-fabricated trap column (3 cm × 150 μm, packed with 5 μm spherical diameter Poroshell 300 SB-C8 stationary phase, Agilent Technologies, Santa Clara, CA, USA) was used for sample desalting, and an analytical column (15 cm × 75 μm, packed with 5 μm Poroshell 300 SB-C8 stationary phase) was used for on-line separation of immunoglobulins prior to ionization. Mobile phase A consisted of 0.1% formic acid in 5% ACN and 95% water. Mobile phase B was 0.1% formic acid in 5% water, 47.5% ACN, and 47.5% isopropyl alcohol. Samples (1.7 fmol–2 pmol mAb) were loaded onto a trap column with 5% B at a flow rate of 2.5 μL/min for 15 min. Separation was then performed with a steep linear gradient from 5% B to 30% B over 5 min followed by a shallow linear ramp from 30% B to 60% B over 30 min at a flow rate of 0.3 μL/min.

Mass spectra were acquired with our custom-built 21 T FT-ICR mass spectrometer [24]. The electrospray ionization (ESI) source voltage was 3–4 kV, and heated capillary temperature was 325 °C. Fragmentation was performed by either electron transfer dissociation (ETD) or collision-induced dissociation (CID) in the Velos Pro linear ion trap. CID and ETD were performed as separate LC-MS/MS experiments. The automatic gain control (AGC) target was set at 1 million charges (1E6) for MS^1 (3 million precursor ion charges (3E6) for mixed therapeutic mAbs in a serum sample), 0.75 million charges (7.5E5) for CID MS/MS, and 0.2 million charges (2E5) for ETD MS/MS. AGC for ETD reagent (fluoranthene radical anions) was set to 0.4 million ions (4E5) with ~5 ms injection period prior to reaction with analyte at a ratio of 2:1. An external quadrupole ion storage device was used to accumulate larger ion populations (3 million charges for product ions) with multiple fills from the Velos Pro MS prior to delivery to the ICR cell.

Broadband mass spectra were acquired from m/z range 650–2000 with 0.76 s time-domain acquisition period and two microscans for adalimumab reduced with TCEP or one microscan for other samples, and product ion spectra were acquired from m/z 300–2000 with 0.38 s acquisition period and four microscans. All data were stored as .raw files. All time-domain data were Hanning apodized, zero-filled, and fast Fourier transformed in magnitude mode. Frequency-to-m/z conversion was performed with a two-term calibration equation [25, 26]. Mass calibration was performed with myoglobin (13+ to 24+ charge states) for m/z ranges 290–2000 and 650–2000.

Data Analysis

Data were manually interpreted by use of Xcalibur 2.1 software (Thermo Fisher Scientific), and chi-square values were calculated in R 3.2.1 for isotopologue abundances from light chain, heavy chain, heavy chain Fc/2, and Fd subunits to evaluate the goodness-of-fit to the corresponding simulated mass spectra. Sequence coverage was determined by Xtract deconvolution and fragments matched to the putative sequence by use of ProSight Lite (10 ppm fragment mass tolerance) [27]. Xtract parameters were set as follows: neutral monoisotopic masses generated from deconvolution, fit factor 44%, remainder 25%, resolving power at m/z 400 set to 150,000, S/N threshold 2, Max charge 25 for light chain, heavy chain Fc, and Fd subunits, and 50 for heavy chain. For identification of mixed therapeutic monoclonal antibodies in human serum, ETD and CID spectra were averaged in Xcalibur and exported as .raw files. ETD and CID fragments were deconvolved with ProSightPC 3.0 (ThermoFisher Scientific) embedded THRASH program with the following parameters: minimum signal-to-noise ratio 2, minimum RL value 0.9, maximum mass 24,000 Da, and maximum charge 25. A database containing human proteins (UniProt, November/2016; 20,161 entries) and 31 FDA-approved therapeutic mAb light chains was created, and ProSightPC was used to search the CID and ETD fragment ion mass spectra against that database under "Absolute Mass" mode. The search parameters were: monoisotopic precursor mass type with 2.2 Da tolerance, monoisotopic fragment mass type with 10 ppm tolerance, Δm and disulfide off.

Results and Discussion

Adalimumab Light Chain and Heavy Chain

Figure 2 shows mass spectra for the light chain (top) and heavy chain (bottom) of reduced adalimumab obtained with our 21 T FT-ICR mass spectrometer over ~2 min chromatographic peak width. The mass spectrum (Figure 2a) shows the charge state distribution for the light chain, ranging from 14+ to 32+. The mass scale-expanded segment for the light chain 23+ charge state (Figure 2b) fits closely to the mass spectrum simulated from the known elemental composition with IsoPro 3.1 (https://sites.google.com/site/isoproms/) (isotopologues abundance χ^2 value 0.0058). The experimental mass for the 23+ charge state
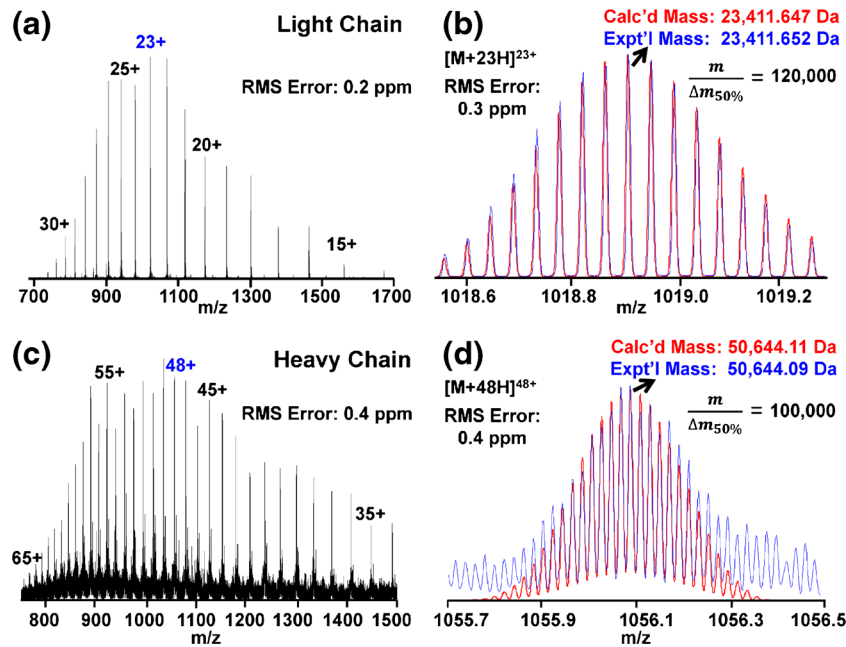
Figure 2. (**a**) Broadband positive-ion ESI 21 T FT-ICR mass spectrum of adalimumab light chain (acquired over 2.2 min of elution, 75 spectra averaged, 2 μS/spectrum). Two pmol adalimumab was loaded onto a nano-LC column; 119 peaks from the seven most abundant charge states were assigned with an RMS error of 0.2 ppm. (**b**) Mass scale-expanded segment for adalimumab light chain 23+ charge state (in blue), fitted to a mass spectrum (in red) simulated from the known elemental composition. The 17 highest-magnitude peaks were assigned with an RMS error of 0.3 ppm. (**c**) Broadband positive-ion ESI 21 T FT-ICR mass spectrum of adalimumab heavy chain (acquired over 2 min of elution, 68 spectra averaged, 2 μS/spectrum). (**d**) Mass scale-expanded segment for adalimumab heavy chain most abundant form (K0G0F) 48+ charge state (in blue), fitted to a mass spectrum (in red) simulated from the known elemental composition. The nine highest-magnitude peaks were assigned with an RMS error of 0.4 ppm

highest magnitude peak is 23,411.652 Da, 0.2 ppm (0.005 Da) from the calculated mass, 23,411.647 Da. Furthermore, the 17 highest-magnitude peaks (each at least 6σ higher than RMS baseline noise) from the 23+ charge state were assigned with RMS error of 0.3 ppm, and the 119 peaks from the seven highest magnitude charge states were assigned with RMS error of 0.2 ppm. The RMS error for a single mass spectrum (2 μS/ spectrum) of light chain was 0.2 ppm. The heavy chain charge state distribution (c) ranges from 34+ to 66+. The mass scale-expanded segment for the heavy chain 48+ charge state most abundant form (G0F glycosylation at asparagine 301 without C-terminal lysine, K0G0F) (Figure 2d) fitted closely to the simulated mass spectrum, and the intact heavy chain isotopic distribution extends beyond the distribution calculated from the known sequence, presumably due to e.g., oxidation, disulfide bond reformation, and deamidation (most abundant 17 isotopologue abundances χ^2 value 0.0219). The nine highest magnitude peaks from the 48+ charge state were assigned with RMS error of 0.4 ppm (abundance χ^2 value 0.0031, d), and the 117 peaks from the 13 highest magnitude charge states were assigned with RMS error of 0.4 ppm. The RMS error for a single mass spectrum (2 μS/spectrum) of heavy chain was 0.5 ppm. The 48+ charge state was further isolated for better characterization, with three forms observed (Figure 3): the most abundant form K0G0F, G1F glycosylation without C-terminal lysine (K0G1F), and G0F glycosylation with one C-terminal lysine (K1G0F). The RMS errors were 0.2 ppm and 0.5 ppm

for a single mass spectrum (2 μS/spectrum) of light chain (23+ charge state) and heavy chain (48+ charge state).

CID and ETD MS/MS of Adalimumab Light Chain and Heavy Chain

The adalimumab light chain 24+ charge state was chosen (isolation window width = 15 Th) for CID and ETD fragmentation in the linear ion trap [21]. Normalized collision energies
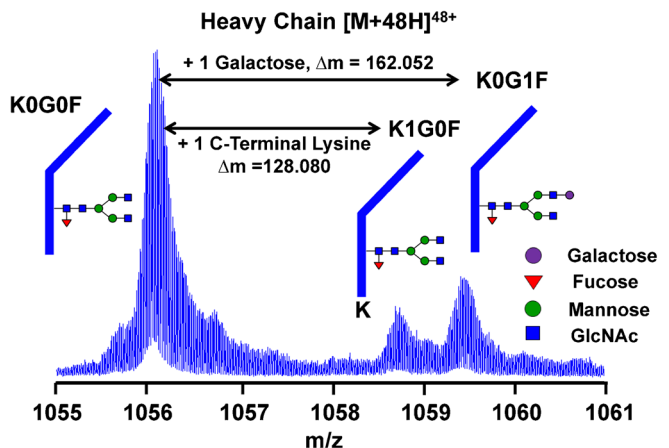

Figure 3. Heavy chain 48+ charge state isolation. Glycosylated forms and C-terminal lysine truncation K0G0F, K1G0F, and K0G1F are indicated

of 35, 40, and 45 with q-activation 0.25 and 0.4 provided the most extensive CID sequence coverage, and activation periods of 3, 5, 10, 15, and 20 ms provided the most extensive ETD coverage. The heavy chain 55+ charge state was selected for fragmentation (isolation window width 15 *Th*). Normalized collision energies of 35, 40, and 45 with q-activation 0.25 were used for CID, and activation periods of 3, 5, 10, and 15 ms for ETD. As shown in Supplementary Figure SI-1, in each case MS/MS generates abundant product fragment ions. The 2.1 min light chain elution window included 44 ETD product ion spectra (2.9 s/spectrum) and 124 CID product ion spectra (1.0 s/spectrum). The 1.9 min heavy chain elution window included 32 ETD product ion spectra (3.6 s/spectrum) and 56 CID product ion spectra (2.0 s/spectrum).

Figure 4 shows fragmentation maps for the adalimumab light chain and heavy chains. Amino acid sequence coverages for adalimumab light and heavy chain, based on combined results from eight targeted nano-LC FT-ICR MS/MS
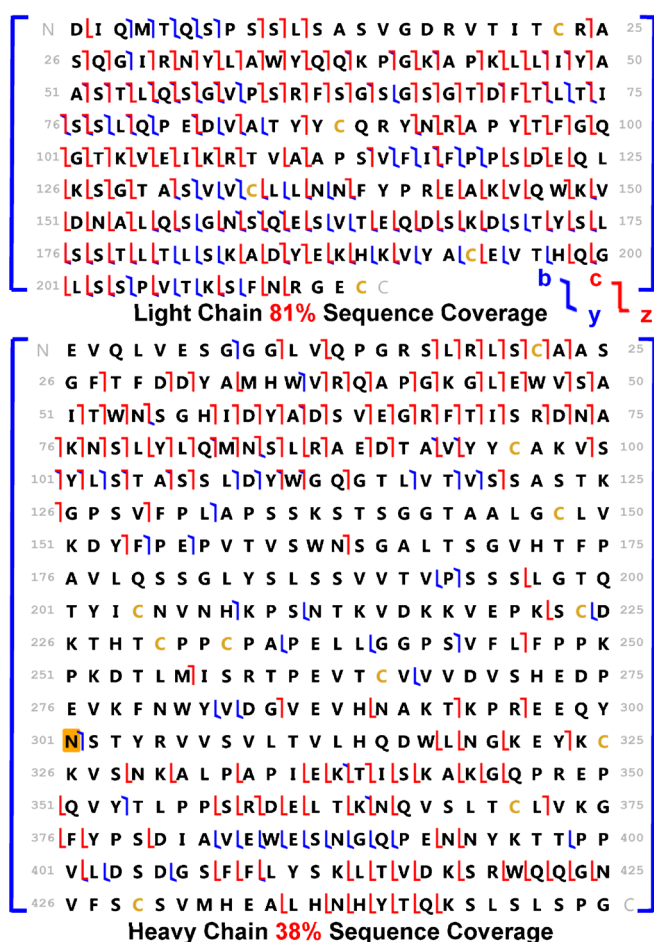
experiments with various collision energies and ETD activation periods, were 81% for light chain and 38% for heavy chain. Extensive cleavage is evident for the variable regions of both light and heavy chains, and the heavy chain N-glycosylation site is localized. Supplementary Figures SI-2 and SI-3 show the assigned fragment RMS mass errors for the light chain (2.9 ppm for 498 assigned CID fragments and 3.0 ppm for 474 assigned ETD fragments) and the heavy chain (4.7 ppm for 101 assigned CID fragments and 4.1 ppm for 242 assigned ETD fragments). Amino acid sequence coverages based on one targeted nano-LC FT-ICR MS/MS experiment with ETD fragmentation (activation period 10 ms) and one targeted nano-LC FT-ICR MS/MS experiment with CID (collision energy 45 with q-activation 0.25) were 66% for light chain and 22% for heavy chain (Supplementary Figure SI-4).

IdeS-Digested Adalimumab Subunits

IdeS digestion of adalimumab followed by TCEP reduction yields three unique fragments: the Fc/2 fragment containing the heavy chain constant region, the Fd fragment containing the heavy chain variable region, and the light chain (see Figure 1). Figure 5 shows the total ion current (TIC) chromatogram for 0.25 pmol IdeS-digested and TCEP-reduced adalimumab. The three subunits are chromatographically baseline-separated, with baseline-resolved broadband mass spectral isotopic distributions (charge states 18+ to 34+). The light chain is the largest area mass spectral peak, followed by Fc/2 and Fd. The difference in ion abundance between light chain and heavy chain subunits may be caused by incomplete IdeS digestion, and the difference between abundances of Fc/2 and Fd subunits could result from different ionization efficiency. The isotopic distributions for the Fc/2 and Fd 28+ charge states fit (isotopologue abundances χ^2 value 0.0037 and 0.0095) those simulated from the known elemental compositions (Figure 6, top). The experimental mass for the Fc/2 and Fd 28+ charge state highest magnitude peaks are 25203.532 Da and 25457.562 Da, deviating by only –0.1 ppm (–0.002 Da) and –0.3 ppm (–0.008 Da) from their corresponding calculated masses. The 17 highest-magnitude peaks for the 28+ charge state were assigned with RMS error of 0.3 ppm for both subunits. Finally, the 119 peaks from the seven highest-magnitude charge states were assigned with RMS error of 0.4 ppm, 0.3 ppm, and 0.3 ppm for Fc/2, LC, and Fd. The RMS errors for a single mass spectrum (1 µS/spectrum) of Fc/2 (28+ charge state), light chain (26+ charge state), and Fd (28+ charge state) were 0.4 ppm.

The 28+ charge state of the adalimumab heavy chain Fc/2 and Fd fragments generated by digestion with IdeS were chosen (isolation window width 15 *Th*) for CID and ETD fragmentation, with normalized collision energies of 35, 40, and 45 with q-activation 0.25 for CID, and activation period ranging from 3 to 20 ms for ETD. The 1.5 min Fc/2 elution window included 32 ETD product ion spectra (2.9 s/spectrum) and 80 CID product ion spectra (1.1 s/spectrum). The 1.3 min Fd elution window included 24 ETD spectra (3.3 s/spectrum) and 60 CID product
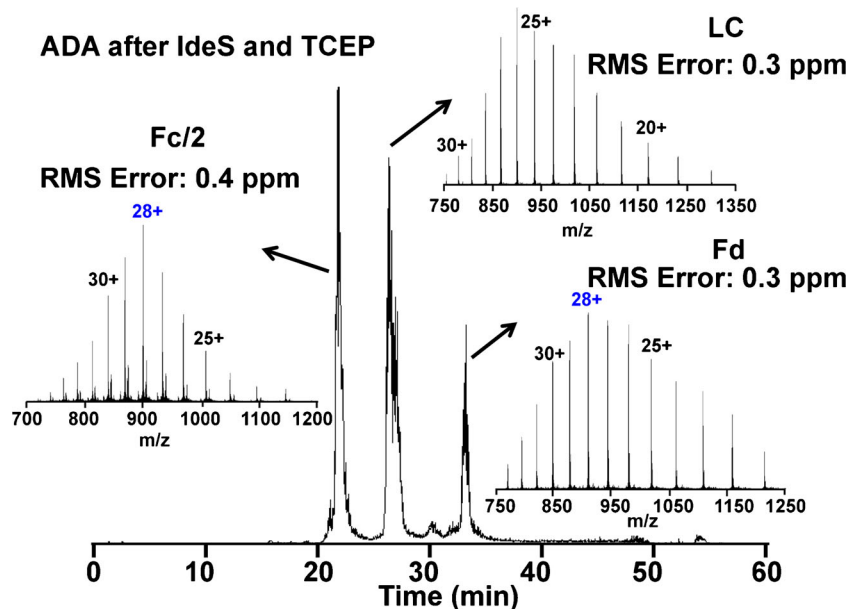

Figure 4. Amino acid sequence coverage for adalimumab light chain (top) and heavy chain (bottom), based on combined results from eight targeted nano-LC FT-ICR MS/MS experiments for light chain 24+ charge state and heavy chain 55+ charge states with various collision induced dissociation collision energy and ETD activation periods (see text)

Figure 5. Total ion current chromatogram for adalimumab subunits after IdeS digestion and TCEP reduction. Broadband (+) ESI 21 T FT-ICR mass spectra of adalimumab Fc/2 (58 spectra averaged, 1 μS/spectrum), light chain (98 spectra averaged, 1 μS/spectrum), and Fd (39 spectra averaged, 1 μS/spectrum) charge state distributions are shown in insets; 0.25 pmol of digested and reduced adalimumab was loaded onto the nano-LC column; 119 peaks from the seven most abundant charge states were assigned with RMS error of 0.4 ppm, 0.3 ppm, and 0.3 ppm for Fc/2, light chain, and Fd
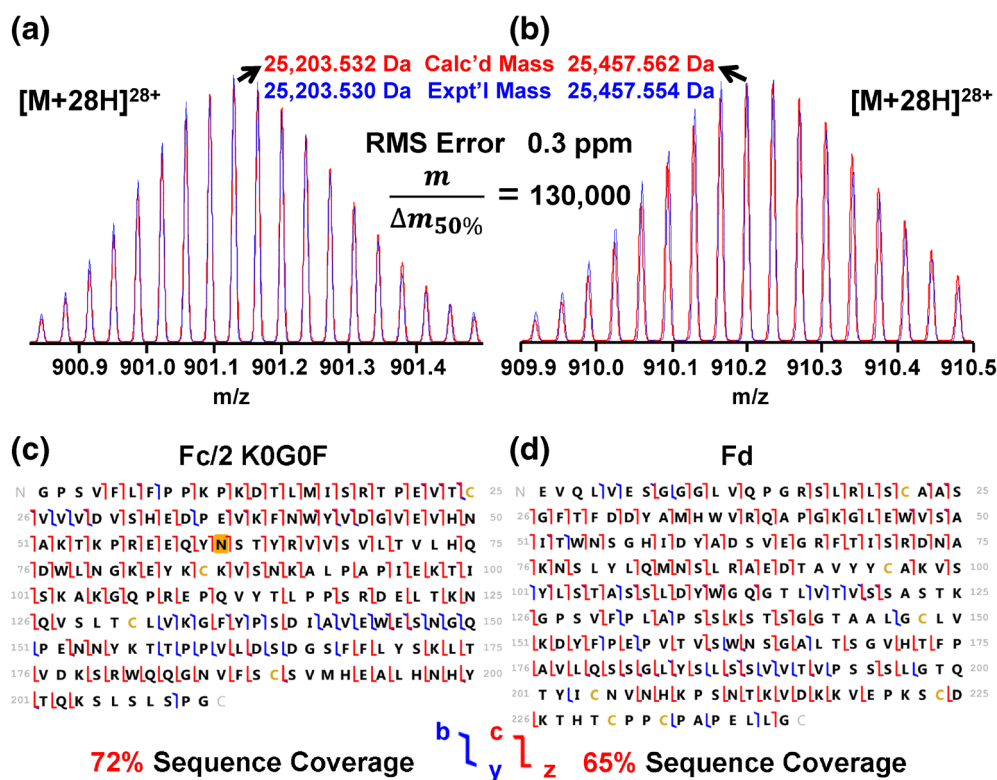
ion spectra (1.3 s/spectrum). Figure 6 (bottom) provides fragmentation maps for adalimumab Fc/2 and Fd subunits. Amino acid sequence coverages based on combined results from eight targeted nano-LC FT-ICR MS/MS experiments with CID (normalized collision energies 35, 40, and 45 with q-activation 0.25) and ETD fragmentation (activation period 3, 5, 10, 15, and 20 ms) were 72% for Fc/2 and 65% for Fd. The assigned fragment mass errors for Fc (Supplementary Figure SI-5) were 2.9 ppm for 160 assigned CID fragments, and 3.1 ppm for 386 assigned ETD fragments, and for the heavy chain Fd (Supplementary Figure SI-6) were 3.0 ppm for 117 assigned CID fragments, and 3.3 ppm for 337 assigned ETD fragments. Amino acid sequence coverages based on a single ETD spectrum (activation period 10 ms, 4 μS) were 37% for Fc/2, 45% for light chain, and 39% for Fd. A single LC-MS/MS run with three ETD activation periods 5 ms, 10 ms, and 15 ms yielded sequence coverage of 58%, 61%, and 50% for Fc/2, light chain, and Fd. After combining the result from a second LC-MS/MS run with CID (normalized collision energy 45 with q-activation 0.25 and 0.4), the corresponding sequence coverages were 68%, 70%, and 59% (Supplementary Figure SI-7).

Adalimumab Spiked into Human Serum as a Model for Patients with a Monoclonal Gammopathy

Monoclonal gammopathy is a term used to describe a B cell proliferative disorder characterized by a plasma cell clonal expansion. If there is clinical suspicion of a monoclonal gammopathy, serum and urine are tested for the presence of elevated levels of a monoclonal immunoglobulin secreted by clonal plasma cells [28–30]. The mAb concentration is below 30 g/L (204 μM) in monoclonal gammopathy of undetermined significance (asymptomatic, monitored yearly for multiple myeloma prognosis), and from 30 g/L (204 μM) to >70 g/L (476 μM) in multiple myeloma [31]. The current clinical laboratory methods for detecting serum monoclonal antibodies include serum protein electrophoresis (SPEP) and immunofixation electrophoresis (IFE) with detection limit of ~0.3 g/L (2 μM) [32]. Recently, Barnidge et al. developed an LC-ESI Q-TOF MS-based platform for the rapid detection, quantification, and isotyping of monoclonal immunoglobulins from patients with monoclonal gammopathy [33]. Clonal plasma cells secrete identical immunoglobulins, each with the same amino acid sequence and, thus, the same molecular mass, enabling them to be monitored by mass spectrometry [34–42].

The work presented here employs adalimumab spiked into human serum as a model for a monoclonal gammopathy biomarker assay, based on the exceptional separation, resolution, mass measurement accuracy, and sensitivity of nano-LC FT-ICR MS/MS. Figure 7a shows the mass spectra averaged over the known 0.5 min elution time window for the light chain from adalimumab taken from an injection of normal serum without adalimumab added. The mass spectrum exhibits a broad range of unresolved peaks representing the normal kappa and lambda polyclonal light chain background [43]. In contrast, serum

(a)

[M+28H]²⁸⁺ — $[M+28H]^{28+}$

25,203.532 Da Calc'd Mass 25,457.562 Da
25,203.530 Da Expt'l Mass 25,457.554 Da

RMS Error 0.3 ppm

$$\frac{m}{\Delta m_{50\%}} = 130{,}000$$

(b)

$[M+28H]^{28+}$

900.9 901.0 901.1 901.2 901.3 901.4
m/z

909.9 910.0 910.1 910.2 910.3 910.4 910.5
m/z

(c) Fc/2 K0G0F

N G P S V F L F P P K P K D T L M I S R T P E V T C 25
26 V L V V D V S H E D P E V K F N W Y V D G V E V H N 50
51 A K T K P R E E Q Y N S T Y R V V S V L T V L H Q 75
76 D W L N G K E Y K C K V S N K A L P A P I E K T I 100
101 S K A K G Q P R E P Q V Y T L P P S R D E L T K N 125
126 Q V S L T C L V K G F Y P S D I A V E W E S N G Q 150
151 P E N N Y K T T P P V L D S D G S F F L Y S K L T 175
176 V D K S R W Q Q G N V F S C S V M H E A L H N H Y 200
201 T Q K S L S L S P G C

72% Sequence Coverage

(d) Fd

N E V Q L V E S G G G L V Q P G R S L R L S C A A S 25
26 G F T F D D Y A M H W V R Q A P G K G L E W V S A 50
51 I T W N S G H I D Y A D S V E G R F T I S R D N A 75
76 K N S L Y L Q M N S L R A E D T A V Y Y C A K V S 100
101 Y L S T A S S L L D Y W G Q G T L V T V S S A S T K 125
126 G P S V F P L A P S S K S T S G G T A A L G C L V 150
151 K D Y F P E P V T V S W N S G A L T S G V H T F P 175
176 A L V L Q S S G L Y S L S S V V T V P S S S L G T Q 200
201 T Y I C N V N H K P S N T K V D K K V E P K S C D 225
226 K T H T C P P C P A P E L L G C

b ⌐ c
  ⌐y ⌐z

65% Sequence Coverage

Figure 6. Top: mass scale-expanded segments for adalimumab heavy chain Fc/2 (**a**) and Fd 28+ charge state (**b**) in blue, each fitted to a mass spectrum (in red) simulated from their known elemental compositions. The 19 and 17 highest-magnitude peaks were assigned with an RMS error of 0.3 ppm for both Fc/2 and Fd. Bottom: amino acid sequence coverage for adalimumab heavy chain Fc/2 (**c**) and Fd (**d**), based on combined results from eight targeted nano-LC FT-ICR MS/MS experiments for the 28+ charge state with various collision induced dissociation collision energies and ETD activation periods (see text)

spiked with 16.9 μM (2.5 g/L) adalimumab (Figure 7b) exhibits a clearly defined multiply charged protein (adalimumab) signal. The peaks from the seven highest-magnitude charge states were assigned with an RMS error of 0.4 ppm. Two targeted nano-LC FT-ICR MS/MS experiments were performed for the multiple myeloma model: one LC-MS/MS for CID with normalized collision energy of 40 with q-activation 0.25 and one LC-MS/MS for ETD with activation period of 10 and 20 ms. Figure 7c displays the light chain fragmentation map with 53% amino acid sequence coverage, based on combined results from two targeted nano-LC FT-ICR MS/MS experiments. The RMS mass error for 74 assigned CID fragments was 3.8 ppm, and for the 105 assigned ETD fragments was 3.3 ppm. Fragment ions generated by MS/MS of the light chain clearly match portions of both the variable region (in green, 54% sequence coverage) and the constant region of adalimumab.

We further tested the sequence coverage for serum spiked with lower amounts of adalimumab. The sequence coverage (Supplementary Figure SI-8) decreased from 40% to 30% when the adalimumab concentration in serum decreased from 1.3 μM (0.2 g/L, 33 fmol mAb loaded) to 0.35 μM (0.05 g/L, 8

fmol loaded) based on two targeted LC-MS/MS experiments (ETD 10 ms and CID normalized collision energy 35, q = 0.25). Thus, FT-ICR MS/MS can characterize mAb sequences even at low concentration, corresponding to the levels found in patient response after treatment.

To assess the prospects for quantifying the light chain of adalimumab in a normal pooled serum matrix containing polyclonal light chains, we spiked adalimumab into normal serum at each of the following concentrations: 0.20 μM (0.03 g/L), 0.41 μM (0.06 g/L), 0.82 μM (0.12 g/L), 1.7 μM (0.25 g/L), 3.4 μM (0.50 g/L), 6.8 μM (1.00 g/L), 13.5 μM (2.00 g/L), and 16.9 μM (2.50 g/L). For normal serum spiked with 0.20 μM adalimumab (1.7 fmol loaded on column), the signal-to-noise ratio for the adalimumab light chain 26+ charge state highest-magnitude isotopic peak was 14. Each broadband FT-ICR mass spectrum of adalimumab light chain was deconvolved with respect to both charge state and isotopic distribution, and the logarithm of deconvolved magnitude-mode peak height plotted as a function of logarithm of concentration (Figure 7d), yielding a highly linear calibration curve ($r^2 = 0.99$). Compared with conventional mAb detection methods (SPEP, IFE), this
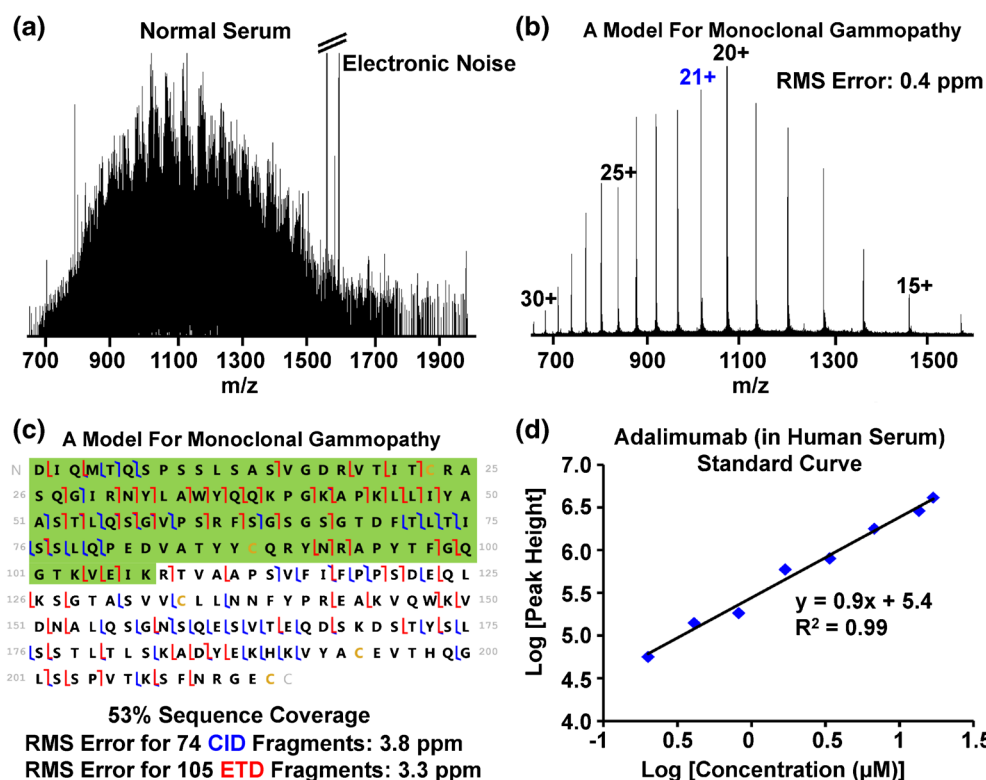
Figure 7. Mass spectra from a normal human serum (**a**) and normal human serum spiked with 15 µM of adalimumab (**b**), a model for monoclonal gammopathy, sample containing 1 pmol adalimumab loaded onto a nano-LC column). The normal human serum mass spectrum shows a broad range of unresolved peaks, whereas the model for monoclonal gammopathy displays a clearly defined multiply charged protein (adalimumab) signal; 119 peaks from the seven highest-magnitude charge states were assigned with an RMS error of 0.4 ppm. (**c**) Amino acid sequence coverage for adalimumab light chain for the monoclonal gammopathy model, based on one targeted nano-LC FT-ICR MS/MS CID and one targeted nano-LC FT-ICR MS/MS ETD experiment. The variable region sequence (in green) differentiates adalimumab from other monoclonal immunoglobulins, and the remaining constant region sequence identifies adalimumab light chain isotype as kappa. (**d**) Adalimumab (in human serum) quantitation generated with our nano-LC FT-ICR MS method (see text)

nano-LC FT-ICR MS approach has the advantage of 10 times lower limit of detection. The lower limit of detection aids early diagnosis of disease and can be used to monitor the patient response after treatment (low mAb concentration in serum). Also, mAb can be quantified for multiple myeloma progression monitoring.

Identification of Mixed Therapeutic Monoclonal Antibodies in Human Serum

To demonstrate the feasibility of the present approach for monitoring the mAbs mixture in serum (a model for the monoclonal gammopathy case when more than one plasma cell clone exists), we analyzed normal human serum spiked with a mixture of five therapeutic monoclonal antibodies (1.3 µM for each mAb, 33 fmol of each mAb loaded on column). Our group was blind to the identity of the therapeutic mAbs present in the serum prior to analysis. One LC-MS was first performed to

analyze the light chain elution and charge state distribution for 5 mAbs. Supplementary Figure SI-9 shows extracted ion chromatograms for the most abundant charge state for each of the five mAbs. For data acquisition, the 5 mAbs were divided into two groups (mAb 1, 3, 5 in group 1; mAb 2, 4 in group 2) based on their LC elution times (mAb2 and mAb3 co-eluted and thus were divided into two groups). Four LC-MS/MS experiments were performed: two to target precursors from group 1 with CID (normalized collision energy 35 and q-activation 0.25) and then with ETD (10 ms) fragmentation and two to target precursors from group 2 (again for CID and ETD fragmentation).

ProSightPC was used to search for ETD and CID fragments against a database constructed from the UniProt human protein database (20,161 entries) to which the sequences of 31 FDA-approved therapeutic mAb light chains were added. The 5 mAbs were correctly identified by ETD or CID as rituximab (mAb1), adalimumab (mAb2), vedolizumab (mAb3), infliximab (mAb4), and eculizumab (mAb5) in each case as the highest scoring result.

Only mAb 2 returned more than one search result, and the second result was easily differentiated from the top search result based on accurate mass and variable region ETD/CID fragments, even though the calculated mass difference was only 1.5 ppm and sequence similarity was 94% between the top and the second highest scoring search results (Figure 8). The corresponding expectation values (E-values) for the 5 mAbs were 2.42E-39, 2.61E-69, 1.73E-67, 1.16E-69, and 1.57E-45 based on ETD fragment search, and 8.14E-22, 9.93E-39, 5.28E-31, 2.25E-34, and 4.95E-31 based on CID fragment search. The matched product ions yielded sequence coverages of 37%, 50%, 42%, 47%, 33% for rituximab, adalimumab, vedolizumab, infliximab, and eculizumab. The corresponding variable region sequence coverages were 21%, 39%, 28%, 36%, and 19% (Supplementary Figure SI-10). The numbers of matched CID and ETD product ions for the light chains of the five spiked mAbs were 69 and 50 for rituximab, 110 and 79 for adalimumab, 80 and 68 for vedolizumab, 109 and 69 for infliximab, and 57 and 53 for eculizumab.

Table 1 shows the most abundant isotopologue mass error and the RMS mass measurement error (~0.2 ppm) from 17 isotopologues from one charge state, along with the sequence coverage for each mAb light chain after search of the customized database.

Adalimumab
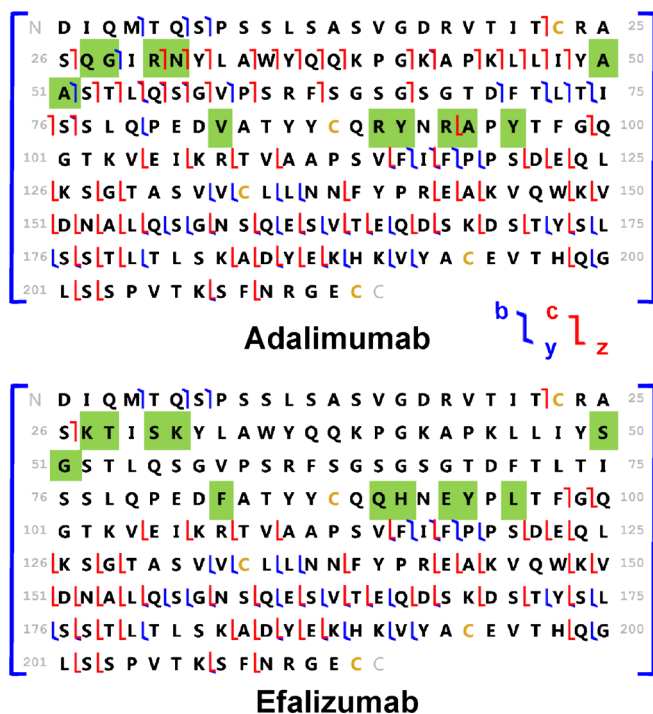
Efalizumab

Figure 8. Sequence comparison between adalimumab and efalizumab light chains. Two hundred two identical amino acids (out of 214 amino acids) yields 94% sequence similarity. The 12 variable region amino acids (in green) differentiate adalimumab from efalizumab. The mass difference between these two light chains is 1.5 ppm

Mass Errors from the Software Deconvolution Algorithm

We note that RMS mass errors for antibody subunit MS^1 and MS/MS fragments were surprisingly different (0.2–0.4 ppm versus 2.9–4.7 ppm). One difference is that MS^1 mass errors were determined from fitting the experimental mass spectrum to the mass spectrum simulated from antibody subunit known elemental composition, whereas MS/MS fragment mass errors were based on the mass difference between the assigned fragments and the calculated averagine distribution fitted to the observed isotopic distribution by the Xtract or THRASH algorithm. When antibody MS1 spectra were deconvolved with Xtract, the neutral monoisotopic mass errors for light chain (75 spectra averaged, two μscans/spectrum), heavy chain (68 spectra averaged, two μscans/spectrum), heavy chain Fc/2 (58 spectra averaged, one μscan/spectrum), and Fd subunits (39 spectra averaged, one microscans/spectrum) were 1.3 ppm, 1.1 ppm, 1.4 ppm, and 1.7 ppm: i.e., ~3–5 times higher mass error than the corresponding broadband mass spectra RMS errors (0.2–0.4 ppm) before deconvolution.

Manual examination of fragment monoisotopic masses (before deconvolution) yielded 0.3 ppm RMS mass error, and the same fragments were assigned with 3.3 ppm RMS mass error after software (Xtract and THRASH) deconvolution (Table 2). The current software deconvolution algorithm generates monoisotopic mass based on the molecular formula of averagine whose distribution is matched to the experimental mass spectrum, and the difference between the molecular formula of fitted averagine and protein/fragments leads to potentially high mass errors [44, 45]. Therefore, future software deconvolution algorithm improvement is needed to match the sample/fragment low mass errors from 21 T FT-ICR MS/MS.

The fragment RMS mass error (~4 ppm after deconvolution) provided correct identifications of proteins in our identification of mixed therapeutic monoclonal antibodies in human serum. However, fragment identification with lower mass errors (e.g., <1 ppm) will greatly improve protein assignment accuracy. For example, the mass differences for fragments c99, b116, b117, b118 between adalimumab and efalizumab (Figure 8) are ~3 ppm (0.03 Da), and a search window width less than 1 ppm will enable accurate assignment of the observed fragments—critical for future database searching and de novo sequencing.

Conclusion

Nano-LC 21 T FT-ICR MS/MS provides comprehensive analysis of monoclonal immunoglobulins with ultrahigh mass

Table 1. Sequence Coverages and Mass Differences Between Experimental and Calculated Mass Spectra for Therapeutic Monoclonal Immunoglobulins Identified by ProSightPC Search

mAb	ProSightPC search		17 Peaks Rms error (ppm)	Most abundant isotopologue		
	Highest score	Sequence coverage		Calc'd mass (Da)	Expt'l mass (Da)	ppm Error
1	Rituximab	37%	0.19	23039.341	23039.344	0.13
2	Adalimumab	50%	0.18	23411.633	23411.632	0.07
3	Vedolizumab	42%	0.16	23905.827	23905.831	0.15
4	Infliximab	47%	0.21	23438.419	23438.420	0.05
5	Eculizumab	33%	0.27	23134.410	23134.411	0.04

measurement accuracy and broad sequence coverage. Fast, simple, and inexpensive sample preparation (15 min Melon gel, 30 min spin filter cleanup, and 15 min TCEP reduction) enables extensive mapping of endogenous and exogenous immunoglobulins present above the polyclonal background. Using adalimumab as a model for high-abundance endogenous monoclonal immunoglobulin, we demonstrate that the light chain, heavy chain, and heavy chain IdeS-generated fragments can be extensively characterized, including N-glycosylation site localization, and three heavy chain isoforms (K0G0F, K0G1F, and K1G0F) [46]. We further extended the method to demonstrate the ability to quantify the intact light chain from a mAb in a polyclonal background matrix as a model for a patient with monoclonal gammopathy—a first for our nano-LC 21 T FT-ICR MS/MS instrument platform.

Pharma has invested extensively in high resolution, high mass measurement accuracy mass spectrometers for characterizing therapeutic mAbs. These high-end instruments routinely analyze therapeutic mAbs from the initial development state to production. However, most of the published methods describing the characterization of mAbs by use of high resolution mass spectrometers are performed in non-human matrices. The goal of this work was to evaluate the performance of our nano-LC 21 T FT-ICR MS/MS instrument for characterizing a mAb in human serum, in the hope of establishing a protocol for utilizing this unique instrumentation in situations for which mass spectrometers used in clinical laboratories would not suffice. Our findings demonstrate the widespread capabilities of this instrument platform, as evident from the outstanding mass measurement accuracy and extensive MS/MS fragmentation data, enabling confident assignment of therapeutic mAbs in the presence of a polyclonal background. The results shown here serve as a blueprint for future characterization of endogenous mAbs in patients with a variety of immune system disorders that cannot be achieved by gene sequencing alone. The results also represent a successful union of clinical laboratory expertise with a national analytical resource.

Acknowledgements

Table 2. Examples of Adalimumab light chain fragments mass errors from THRASH Deconvolution, Xtract Deconvolution, and Monoisotopic Peaks (before deconvolution). The RMS errors for THRASH deconvolution, Xtract Deconvolution, and Monoisotopic Peaks were 3.3 ppm, 3.3 ppm, and 0.3 ppm

Ion Type	THRASH deconvolution ppm error	Xtract deconvolution ppm error	Monoisotopic peak ppm error
c34	-4.0	3.0	0.4
c35	-6.3	2.7	0.3
c36	-1.6	1.1	0.4
c38	3.8	-4.1	0.4
c45	-2.1	1.0	0.5
c54	-2.7	-1.0	0.2
z30	-3.1	-9.2	0.3
b51	-2.4	2.3	-0.1
y13	-2.8	2.1	0.3
y21	-2.6	2.5	0.3
y27	-1.8	3.1	0.2
y40	-4.0	1.0	0.3
y51	-3.0	2.2	0.1
y54	-3.0	1.7	0.5

References

1. Beck, A., Wurch, T., Bailly, C., Corvaia, N.: Strategies and challenges for the next generation of therapeutic antibodies. Nat. Rev. Immunol. **10**, 345–352 (2010)
2. Ecker, D.M., Jones, S.D., Levine, H.L.: The therapeutic monoclonal antibody market. mAbs **7**, 9–14 (2015)
3. Scott, A.M., Wolchok, J.D., Old, L.J.: Antibody therapy of cancer. Nat. Rev. Cancer. **12**, 278–287 (2012)
4. Chan, A.C., Carter, P.J.: Therapeutic antibodies for autoimmunity and inflammation. Nat. Rev. Immunol. **10**, 301–316 (2010)
5. Bouchard, H., Viskov, C., Garcia-Echeverria, C.: Antibody-drug conjugates—a new wave of cancer drugs. Bioorg. Med. Chem. Lett. **24**, 5357–5363 (2014)
6. Sondermann, P., Szymkowski, D.E.: Harnessing Fc receptor biology in the design of therapeutic antibodies. Curr. Opin. Immunol. **40**, 78–87 (2016)

7. Murray, D., Barnidge, D.: Characterization of immunoglobulin by mass spectrometry with applications for the clinical laboratory. Crit. Rev. Clin. Lab. Sci. **50**, 91–102 (2013)

8. Beck, A., Wagner-Rousset, E., Ayoub, D., Van Dorsselaer, A., Sanglier-Cianferani, S.: Characterization of therapeutic antibodies and related products. Anal. Chem. **85**, 715–736 (2013)

9. Dekker, L., Wu, S., Vanduijn, M., Tolic, N., Stingl, C., Zhao, R., Luider, T., Pasa-Tolic, L.: An integrated top-down and bottom-up proteomic approach to characterize the antigen-binding fragment of antibodies. Proteomics **14**, 1239–1248 (2014)

10. Srzentic, K., Fornelli, L., Laskay, U.A., Monod, M., Beck, A., Ayoub, D., Tsybin, Y.O.: Advantages of extended bottom-up proteomics using Sap9 for analysis of monoclonal antibodies. Anal. Chem. **86**, 9945–9953 (2014)

11. Pang, Y., Wang, W.H., Reid, G.E., Hunt, D.F., Bruening, M.L.: Pepsin-containing membranes for controlled monoclonal antibody digestion prior to mass spectrometry analysis. Anal. Chem. **87**, 10942–10949 (2015)

12. Zhang, L., English, A.M., Bai, D.L., Ugrin, S.A., Shabanowitz, J., Ross, M.M., Hunt, D.F., Wang, W.H.: Analysis of monoclonal antibody sequence and post-translational modifications by time-controlled proteolysis and tandem mass spectrometry. Mol. Cell. Proteom. **15**, 1479–1488 (2016)

13. Gahoual, R., Busnel, J.M., Beck, A., Francois, Y.N., Leize-Wagner, E.: Full antibody primary structure and microvariant characterization in a single injection using transient isotachophoresis and sheathless capillary electrophoresis-tandem mass spectrometry. Anal. Chem. **86**, 9074–9081 (2014)

14. Mukherjee, R., Adhikary, L., Khedkar, A., Iyer, H.: Probing deamidation in therapeutic immunoglobulin gamma (IgG1) by 'bottom-up' mass spectrometry with electron transfer dissociation. Rapid Commun. Mass Spectrom. **24**, 879–884 (2010)

15. Zhang, Z., Pan, H., Chen, X.: Mass spectrometry for structural characterization of therapeutic antibodies. Mass Spectrom. Rev. **28**, 147–176 (2009)

16. Mao, Y., Valeja, S.G., Rouse, J.C., Hendrickson, C.L., Marshall, A.G.: Top-down structural analysis of an intact monoclonal antibody by electron capture dissociation-Fourier transform ion cyclotron resonance-mass spectrometry. Anal. Chem. **85**, 4239–4246 (2013)

17. Fornelli, L., Damoc, E., Thomas, P.M., Kelleher, N.L., Aizikov, K., Denisov, E., Makarov, A., Tsybin, Y.O.: Analysis of intact monoclonal antibody IgG1 by electron transfer dissociation Orbitrap FTMS. Mol. Cell. Proteom. **11**, 1758–1767 (2012)

18. Wang, D., Wynne, C., Gu, F., Becker, C., Zhao, J., Mueller, H.M., Li, H., Shameem, M., Liu, Y.H.: Characterization of drug-product-related impurities and variants of a therapeutic monoclonal antibody by higher energy C-trap dissociation mass spectrometry. Anal. Chem. **87**, 914–921 (2015)

19. Bondarenko, P.V., Second, T.P., Zabrouskov, V., Makarov, A.A., Zhang, Z.: Mass measurement and top-down HPLC/MS analysis of intact monoclonal antibodies on a hybrid linear quadrupole ion trap-Orbitrap mass spectrometer. J. Am. Soc. Mass Spectrom. **20**, 1415–1424 (2009)

20. Zhang, Z., Shah, B.: Characterization of variable regions of monoclonal antibodies by top-down mass spectrometry. Anal. Chem. **79**, 5723–5729 (2007)

21. Fornelli, L., Ayoub, D., Aizikov, K., Beck, A., Tsybin, Y.O.: Middle-down analysis of monoclonal antibodies with electron transfer dissociation orbitrap fourier transform mass spectrometry. Anal. Chem. **86**, 3005–3012 (2014)

22. Cotham, V.C., Brodbelt, J.S.: Characterization of therapeutic monoclonal antibodies at the subunit-level using middle-down 193 nm ultraviolet photodissociation. Anal. Chem. **88**, 4004–4013 (2016)

23. Sjogren, J., Olsson, F., Beck, A.: Rapid and improved characterization of therapeutic antibodies and antibody related products using IdeS digestion and subunit analysis. Analyst **141**, 3114–3125 (2016)

24. Hendrickson, C.L., Quinn, J.P., Kaiser, N.K., Smith, D.F., Blakney, G.T., Chen, T., Marshall, A.G., Weisbrod, C.R., Beu, S.C.: 21 Tesla Fourier transform ion cyclotron resonance mass spectrometer: a national resource for ultrahigh resolution mass analysis. J. Am. Soc. Mass Spectrom. **26**, 1626–1632 (2015)

25. Shi, S.D.H., Drader, J.J., Freitas, M.A., Hendrickson, C.L., Marshall, A.G.: Comparison and interconversion of the two most common frequency-to-mass calibration functions for Fourier transform ion cyclotron resonance mass spectrometry. Int. J. Mass Spectrom. **195**, 591–598 (2000)

26. Ledford Jr., E.B., Rempel, D.L., Gross, M.L.: Space charge effects in Fourier transform mass spectrometry. Mass calibration. Anal. Chem. **56**, 2744–2748 (1984)

27. Fellers, R.T., Greer, J.B., Early, B.P., Yu, X., LeDuc, R.D., Kelleher, N.L., Thomas, P.M.: ProSight Lite: graphical software to analyze top-down mass spectrometry data. Proteomics **15**, 1235–1238 (2015)

28. Agarwal, A., Ghobrial, I.M.: Monoclonal gammopathy of undetermined significance and smoldering multiple myeloma: a review of the current understanding of epidemiology, biology, risk stratification, and management of myeloma precursor disease. Clin. Cancer Res. **19**, 985–994 (2013)

29. Kyle, R.A., Buadi, F., Rajkumar, S.V.: Management of monoclonal gammopathy of undetermined significance (MGUS) and smoldering multiple myeloma (SMM). Oncology (Williston Park) **25**(578–586) (2011)

30. van de Donk, N.W., Mutis, T., Poddighe, P.J., Lokhorst, H.M., Zweegman, S.: Diagnosis, risk stratification and management of monoclonal gammopathy of undetermined significance and smoldering multiple myeloma. Int. J. Lab. Hematol. **38**(Suppl 1), 110–122 (2016)

31. Durie, B.G., Salmon, S.E.: A clinical staging system for multiple myeloma. Correlation of measured myeloma cell mass with presenting clinical features, response to treatment, and survival. Cancer **36**, 842–854 (1975)

32. Jaskowski, T.D., Litwin, C.M., Hill, H.R.: Detection of kappa and lambda light chain monoclonal proteins in human serum: automated immunoassay versus immunofixation electrophoresis. Clin. Vaccine Immunol. **13**, 277–280 (2006)

33. Barnidge, D.R., Dasari, S., Botz, C.M., Murray, D.H., Snyder, M.R., Katzmann, J.A., Dispenzieri, A., Murray, D.L.: Using mass spectrometry to monitor monoclonal immunoglobulins in patients with a monoclonal gammopathy. J. Proteome Res. **13**, 1419–1427 (2014)

34. Botz, C.M., Barnidge, D.R., Murray, D.L., Katzmann, J.A.: Detecting monoclonal light chains in urine: microLC-ESI-Q-TOF mass spectrometry compared to immunofixation electrophoresis. Br. J. Haematol. **167**, 437–438 (2014)

35. Barnidge, D.R., Kohlhagen, M.C., Zheng, S., Willrich, M.A., Katzmann, J.A., Pittock, S.J., Murray, D.L.: Monitoring oligoclonal immunoglobulins in cerebral spinal fluid using microLC-ESI-Q-TOF mass spectrometry. J. Neuroimmunol. **288**, 123–126 (2015)

36. Barnidge, D.R., Krick, T.P., Griffin, T.J., Murray, D.L.: Using matrix-assisted laser desorption/ionization time-of-flight mass spectrometry to detect monoclonal immunoglobulin light chains in serum and urine. Rapid Commun. Mass Spectrom. **29**, 2057–2060 (2015)

37. Mills, J.R., Barnidge, D.R., Murray, D.L.: Detecting monoclonal immunoglobulins in human serum using mass spectrometry. Methods **81**, 56–65 (2015)

38. Barnidge, D.R., Dispenzieri, A., Merlini, G., Katzmann, J.A., Murray, D.L.: Monitoring free light chains in serum using mass spectrometry. Clin. Chem. Lab. Med. **54**, 1073–1083 (2016)

39. Kohlhagen, M.C., Barnidge, D.R., Mills, J.R., Stoner, J., Gurtner, K.M., Liptac, A.M., Lofgren, D.I., Vanderboom, P.M., Diepenzieri, A., Katzmann J.A., Willrich, M.A., Snyder, M.R., Murray, D.L.: Screening method for M-proteins in serum using nanobody enrichment coupled to MALDI-TOF mass spectrometry. Clin. Chem. **62**, 1345–1352 (2016)

40. Leung, N., Barnidge, D.R., Hutchison, C.A.: Laboratory testing in monoclonal gammopathy of renal significance (MGRS). Clin. Chem. Lab. Med. **54**, 929–937 (2016)

41. Mills, J.R., Cornec, D., Dasari, S., Ladwig, P.M., Hummel, A.M., Cheu, M.: Using mass spectrometry to quantify rituximab and perform individualized immunoglobulin phenotyping in ANCA-associated vasculitis. Anal. Chem. **88**, 6317–6325 (2016)

42. Mills, J.R., Kohlhagen, M.C., Dasari, S., Vanderboom, P.M., Kyle, R.A., Katzmann, J.A., Willrich, M.A., Barnidge, D.R., Dispenzieri, A., Murray, D.L.: Comprehensive assessment of M-proteins using nanobody enrichment coupled to MALDI-TOF mass spectrometry. Clin. Chem. **62**, 1334–1344 (2016)

43. Barnidge, D.R., Dasari, S., Ramirez-Alvarado, M., Fontan, A., Willrich, M.A., Tschumper, R.C., Jelinek, D.F., Snyder, M.R., Dispenzieri, A., Katzmann, J.A., Murray, D.L.: Phenotyping polycloncal kappa and lambda light chain molecular mass distributions in patient serum using mass spectrometer. J. Protome Res. **13**, 5198–5205 (2014)

44. Senko, M.W., Beu, S.C., McLaffertycor, F.W.: Determination of monoisotopic masses and ion populations for large biomolecules from resolved isotopic distributions. J. Am. Soc. Mass Spectrom. **6**, 229–233 (1995)

45. Horn, D.M., Zubarev, R.A., McLafferty, F.W.: Automated reduction and interpretation of high resolution electrospray mass spectra of large molecules. J. Am. Soc. Mass Spectrom. **11**, 320–332 (2000)

46. An, Y., Zhang, Y., Mueller, H.M., Shameem, M., Chen, X.: A new tool for monoclonal antibody analysis: application of IdeS protelysis in IgG domain-specific characterization. mAbs **6**, 879–893 (2014)